



# University of HUDDERSFIELD

## University of Huddersfield Repository

Pradhan, Suman and Mishra, Rakesh

Measurement of properties of a dispersed phase in air-water multiphase flow using novel four-sensor probe and orthogonal high speed cameras

### Original Citation

Pradhan, Suman and Mishra, Rakesh (2015) Measurement of properties of a dispersed phase in air-water multiphase flow using novel four-sensor probe and orthogonal high speed cameras. In: FLUVISU 2015, 16th-20th November, Pleumeur-Bodou/Lannion, France. (Unpublished)

This version is available at <http://eprints.hud.ac.uk/id/eprint/26099/>

The University Repository is a digital collection of the research output of the University, available on Open Access. Copyright and Moral Rights for the items on this site are retained by the individual author and/or other copyright owners. Users may access full items free of charge; copies of full text items generally can be reproduced, displayed or performed and given to third parties in any format or medium for personal research or study, educational or not-for-profit purposes without prior permission or charge, provided:

- The authors, title and full bibliographic details is credited in any copy;
- A hyperlink and/or URL is included for the original metadata page; and
- The content is not changed in any way.

For more information, including our policy and submission procedure, please contact the Repository Team at: [E.mailbox@hud.ac.uk](mailto:E.mailbox@hud.ac.uk).

<http://eprints.hud.ac.uk/>

# Measurement of properties of a dispersed phase in air-water multiphase flow using novel four-sensor probe and orthogonal high speed cameras

S. Pradhan<sup>1</sup>, R. Mishra

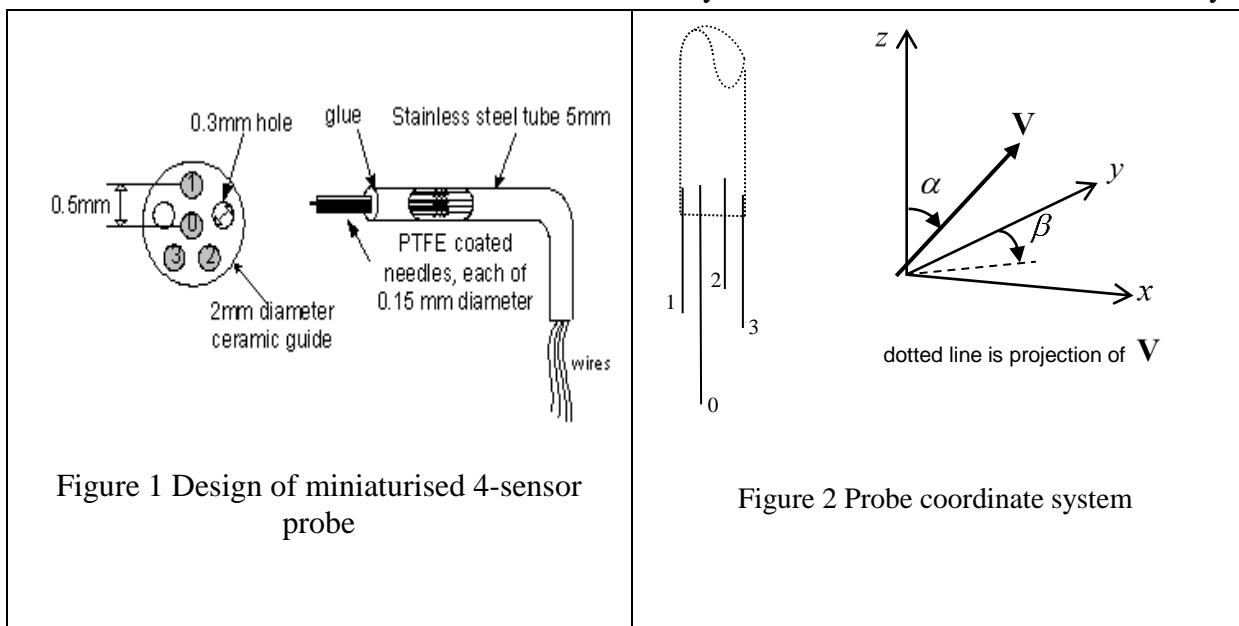
<sup>1</sup> University of Huddersfield, School of Computing and Engineering [S.R.Pradhan@hud.ac.uk](mailto:S.R.Pradhan@hud.ac.uk)

## 1. Introduction

This paper describes further developments related to the ongoing efforts [1-5] to design and perfect a 4-sensor conductance probe for measuring the velocities of individual bubbles in bubbly gas-liquid (and liquid-liquid) flows. In the first part of the paper a new design for a 4-sensor conductance probe is presented which is substantially smaller than previous designs and which therefore reduces bubble-probe interaction effects. The paper then goes on to recapitulate the mathematical model which enables the bubble velocity vector, relative to the probe coordinate system, to be measured in terms of a polar angle  $\alpha$ , an azimuthal angle  $\beta$  and a velocity magnitude  $v$ . Next, the paper goes on to describe a reference measurement system, comprising two high speed cameras, which enable a reference measurement of the bubble velocity vector to be made relative to the  $(x, y, z)$  coordinate system of the water tank in which the experiments are carried out. The image processing theory necessary to extract both the 3-dimensional bubble velocity vector and the bubble shape from the high speed camera images is described in detail. Finally, experimental results are presented for (i) bubble velocity vectors measured by the new miniaturised 4-sensor probe and (ii) bubble trajectories and shapes measured by the high speed camera system.

## 2. Construction of 4-sensor probe and the model for determining the bubble velocity vector

For further scaling down of the 4-sensor probe, PTFE covered stainless steel needles were used. These PTFE covered needles have a moderately small width of 0.15mm and since they



have a protecting PTFE covering there is no requirement for a varnish covering which can roughen the needle surface. To position precisely the four needles utilized as a part of the test, a bored clay aide was utilized as demonstrated as shown in figure 1. The measurements of the

sensor spacing were achieved utilizing an advanced magnifying lens. Mishra et al [1] and Lucas et al [2] have presented a theoretical model which is used to compute various flow properties corresponding to the dispersed phase in typical bubbly air-water flows using the time delay measurements from a four-sensor probe. The developed model is based on the assumptions that the Mathematical model is valid for spherical bubbles, the impact of a bubble on the probe does not affect the bubble's velocity vector and the bubbles do not get deformed during the process of interaction with sensors. Figure 2 shows a schematic diagram of a typical four-sensor probe and the motion of a bubble of radius  $R$  moving with velocity vector  $\mathbf{V}$ . The velocity vector can be represented mathematically as:-

$$\mathbf{V} = v(\sin\alpha\sin\beta\mathbf{i} + \sin\alpha\cos\beta\mathbf{j} + \cos\alpha\mathbf{k}) \quad (1)$$

where  $v$  is velocity magnitude,  $\alpha$  is polar angle between velocity vector and probe axis and  $\beta$  is an azimuthal angle for velocity vector. Lucas et al [2] developed a detailed procedure to calculate polar angle  $\alpha$  and azimuthal angle  $\beta$  of vertically rising bubble from time delay measurements made by the four-sensor probe. The corresponding equations are given below.

$$\tan\beta = \frac{\left(\frac{z_1}{\delta t_{11}} - \frac{z_2}{\delta t_{22}}\right)\left(\frac{y_1}{\delta t_{11}} - \frac{y_3}{\delta t_{33}}\right) - \left(\frac{z_1}{\delta t_{11}} - \frac{z_3}{\delta t_{33}}\right)\left(\frac{y_1}{\delta t_{11}} - \frac{y_2}{\delta t_{22}}\right)}{\left(\frac{z_1}{\delta t_{11}} - \frac{z_2}{\delta t_{22}}\right)\left(\frac{x_1}{\delta t_{11}} - \frac{x_2}{\delta t_{22}}\right) - \left(\frac{z_1}{\delta t_{11}} - \frac{z_2}{\delta t_{22}}\right)\left(\frac{x_1}{\delta t_{11}} - \frac{x_3}{\delta t_{33}}\right)} \quad (2)$$

$$\tan\alpha = \frac{\left(\frac{z_1}{\delta t_{11}} - \frac{z_2}{\delta t_{22}}\right)}{\left(\frac{x_1}{\delta t_{11}} - \frac{x_2}{\delta t_{22}}\right)\sin\beta - \left(\frac{y_1}{\delta t_{11}} - \frac{y_2}{\delta t_{22}}\right)\cos\beta} \quad (3)$$

$$\frac{v\delta t_{ii}}{2} = x_i\sin\alpha\sin\beta + y_i\sin\alpha\cos\beta + z_i\cos\alpha \quad (4)$$

Velocity magnitude  $v$  can be calculated using equation 4, where  $\delta t_{ii}$  represents the time interval between the contacts of the front sensor and  $i^{\text{th}}$  rear sensor with the bubble,  $x_i, y_i$  and  $z_i$  are coordinate of  $i^{\text{th}}$  rear sensor with respect to front sensors.

### 3. Image processing

In this section a model is described which enables determination of the reference velocity vector of an individual bubble, relative to the coordinate system  $(x, y, z)$  of the tank, from images from 2 orthogonal high speed cameras. The model also enables mathematical expressions to be obtained for the shape of a given bubble. Although the model is able to provide a reference velocity vector for any part of the bubble (e.g. the geometric centre of the upper or lower surface, the centre of gravity etc.) it was subsequently found that, due to oscillations of the bubble surface, the most useful reference velocity vector was that of the bubble centre of gravity. The analysis presented in this section is applied to images taken by camera 1, which is orthogonal to the  $x, z$  plane of the tank coordinate system, and by camera 2 which is orthogonal to the  $y, z$  plane of the tank coordinate system. The camera images were pre processed such that pixels which correspond to points on the bubble boundary were readily identifiable. The analysis given below is for a bubble image from camera 1 only. A similar analysis was undertaken for the bubble image from camera 2. It is assumed that the bubble image from camera 1 (orthogonal to the  $x, z$  plane) is in the shape of two semi-

ellipses with a common major axis of length  $a_T$ . The bubble centre of gravity (COG) is at the centre of this major axis which is assumed to be the longest possible chord between any two boundary points of the bubble. Assume that points  $(x_1, z_1)$  and  $(x_2, z_2)$  represent the end points of the major axis. The bubble centre of gravity then has coordinates  $(x_c, z_c)$  where

$$(x_c, z_c) = \frac{(x_2 - x_1)}{2}, \frac{(z_2 - z_1)}{2} \quad (5)$$

The slope  $m_1$  of the major axis is given by  $m_1 = \frac{(z_2 - z_1)}{(x_2 - x_1)}$  (6)

The slope  $m_2$  of the minor axis of the semi-ellipse forming the top half of the bubble is obtained from the relationship  $m_1 m_2 = -1$  and from this calculated value of  $m_2$  we can now initially assume that the semi-ellipse defining the top half of the bubble passes through point  $\mu$  (see figure 3) where the coordinates of  $\mu$  are the intersection of the line of slope  $m_2$  (which passes through the centre of the major axis) and the upper boundary of the bubble image. From the coordinates of  $\mu$  it is now possible to make an initial guess for the length  $b_T$  of the minor axis for the semi-ellipse defining the top of the bubble. At this stage it is helpful to define a new coordinate system  $(\tilde{x}, \tilde{z})$  such that  $\tilde{x} = x - x_c$  and  $\tilde{z} = z - z_c$ . Suppose the major axis of the ellipse makes an angle  $\phi$  with the increasing  $\tilde{x}$  axis as shown in figure 3. We may define another new coordinate system  $(\hat{x}, \hat{z})$  such that  $\hat{x} = \tilde{x} \cos \phi + \tilde{z} \sin \phi$  and  $\hat{z} = -\tilde{x} \sin \phi + \tilde{z} \cos \phi$ . In the  $(\hat{x}, \hat{z})$  coordinate system the equation for the initial guess of the semi-ellipse forming the top half of the bubble is (for positive  $\hat{z}$  only)

$$\frac{\hat{x}^2}{a_T^2} + \frac{\hat{z}^2}{b_T^2} = 1 \quad (7)$$

#### 4 Mathematical models of bubble velocity vector using cameras

The curve of the semi-ellipse created from equation 7 is not necessarily the best fit to the boundary points for the top half of the bubble image obtained from camera 1 therefore it is necessary to use least squares curve fitting to minimize the distance of the boundary points in the bubble image from the calculated bubble boundary. This curve fitting is carried out in the  $\hat{x}, \hat{z}$  coordinate system, where the origin is at the COG of the bubble, where the  $\hat{x}$  axis coincides with the bubble major axis and where the  $\hat{z}$  axis coincides with the minor axis of the top part of the bubble. Let us define a point  $\omega_i$  with coordinates  $(\hat{x}_i, \hat{z}_i)$  which lies on the boundary of the upper part of the image of the bubble (figure 3). We may also define a line with gradient  $\hat{m}_i$  from the COG of the ellipse to  $\omega_i$ . This line intersects the boundary of the calculated ellipse at point  $\lambda_i$  with coordinates  $(\hat{x}'_i, \hat{z}'_i)$  (figure 3). We may calculate  $\hat{x}'_i$  and  $\hat{z}'_i$  as follows. From equation 6, we have

$$\left(\frac{\hat{x}'_i}{a_T}\right)^2 + \left(\frac{\hat{z}'_i}{b_T}\right)^2 = 1 \quad (8)$$

But we also have the relationship that  $\hat{z}'_i = \hat{m}_i \hat{x}'_i$  and so we have that

$$\hat{x}'_i = \sqrt{a_T^2 b_T^2 / (b_T^2 + \hat{m}_i^2 a_T^2)} \quad \text{and} \quad \hat{z}'_i = \hat{m}_i \sqrt{a_T^2 b_T^2 / (b_T^2 + \hat{m}_i^2 a_T^2)} \quad (9)$$

The distance from the COG to  $\lambda_i$  is  $s_i$  and the distance from the COG to  $\omega_i$  is  $r_i$  where

$$r_i = \sqrt{(\hat{x}'_i)^2 + (\hat{z}'_i)^2} \quad \text{and} \quad s_i = \sqrt{(\hat{x}'_i)^2 + (\hat{z}'_i)^2} \quad (10)$$

$$\text{We may define an error term } \varepsilon_i \text{ such that } \varepsilon_i = (s_i - r_i)^2 \quad (11)$$

$$\text{A total error term } \varepsilon \text{ can now be defined such that } \varepsilon = \sum_{i=1}^N \varepsilon_i \quad (12)$$

where  $N$  is the number of individual points (pixels) on the upper part of the bubble boundary in the image from camera 1. By minimising  $\varepsilon$  we can find the best value for  $b_T$ , the length of the minor axis of the semi-ellipse which defines the upper part of the bubble boundary in the image from camera 1. A similar procedure is followed to find the best value for  $b_B$  the length of the minor axis of the semi-ellipse for the bottom part of the bubble image from camera 1. The whole procedure is then repeated for the image from camera 2. Once optimum values for the major and minor axes of all of the relevant semi-ellipses have been found the appropriate ellipse equations are transformed back into the  $(x, y, z)$  coordinate system. For successive images of the bubble from camera 1, separated by a time interval  $\delta t$ , we may calculate bubble velocity components  $v_x$  and  $v_{z,1}$  where

$$v_x = \frac{\delta x}{\delta t} \quad \text{and} \quad v_{z,1} = \frac{\delta z_1}{\delta t} \quad (13)$$

and where  $\delta x$  and  $\delta z_1$  are the displacements of the bubble COG in the  $x$  and  $z$  directions respectively, as viewed by camera 1. Similarly for camera 2 we may define bubble velocity components  $v_y$  and  $v_{z,2}$  where

$$v_y = \frac{\delta y}{\delta t} \quad \text{and} \quad v_{z,2} = \frac{\delta z_2}{\delta t} \quad (14)$$

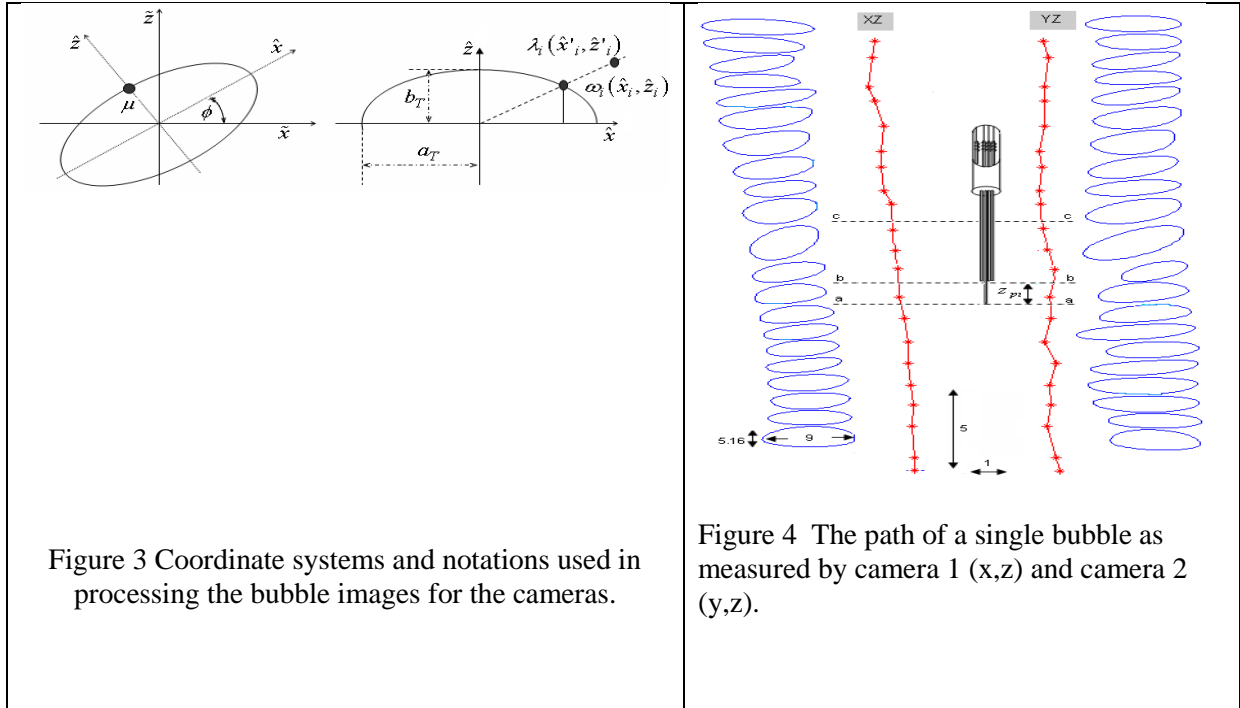
We can now define a bubble velocity vector  $\mathbf{V}_{bt}$  relative to the tank where

$$\mathbf{V}_{bt} = v_x \mathbf{i} + v_y \mathbf{j} + v_z \mathbf{k} \quad (15)$$

$$\text{and where } v_z = (v_{z,1} + v_{z,2})/2 \quad (16)$$

## 5. Experimental results

In figure 4 depicts the trajectory of the centre of gravity of a bubble injected from the base of a water tank in which the 4-sensor probe was mounted 500mm above the injection system. The figure shows the bubble trajectory in the  $x, z$  plane of the water tank, as measured by camera 1, and  $y, z$  plane, as measured by camera 2. Furthermore, figure 4 also shows the outline shapes of the bubble as viewed in the  $x, z$  and  $y, z$  planes for each of the bubble position. From results, the initial assumption was made that the velocity vector of each bubble relative to the tank was purely in the vertical direction.



Given this simplifying assumption, the angles  $\alpha^*$  and  $\beta^*$  by which the probe is rotated relative to the tank coordinate system now represent ‘reference values’ for the polar and azimuthal angles  $\alpha$  and  $\beta$  of the bubble velocity vector  $\mathbf{V}$  relative to the probe coordinate system. Thus  $\alpha_{ref} = \alpha^*$  and  $\beta_{ref} = \beta^*$ . The reference velocity magnitude  $v_{ref}$  of the bubble velocity vector relative to the probe coordinate system is given by  $v_{ref} = v_z$  where  $v_z$  is obtained from equation 16 using data from cameras 1 and 2.

Table 2 Values of polar angle, azimuthal angle and velocity magnitude measured by the probe, and reference values for these quantities

	$\alpha_{ref}$	$\beta_{ref}$	$v_{ref}$	$\alpha_{meas}$	$\beta_{meas}$	$v_{meas}$
Test no.	(deg)	(deg)	( $\text{ms}^{-1}$ )	(deg)	(deg)	( $\text{ms}^{-1}$ )
1	0	N/A	0.38	4.44	N/A	0.37
2	0	N/A	0.38	7.50	N/A	.38
3	0	N/A	0.38	2.73	N/A	0.41
4	10	0	0.41	9.01	337.66	0.39
5	10	90	0.41	9.98	82.04	0.44
6	10	180	0.41	6.13	177.65	0.42
7	20	0	0.35	22.41	7.27	0.36

8	20	0	0.35	20.49	16.44	0.36
9	20	180	0.35	19.17	188.31	0.33

A series of measurements were carried out using the 4-sensor probe to obtain values of  $\alpha_{meas}$ ,  $\beta_{meas}$  and  $v_{meas}$ . These measurements were made for ranges of values of  $\alpha_{ref}$  and  $\beta_{ref}$ . Values of  $\alpha_{meas}$ ,  $\beta_{meas}$  and  $v_{meas}$  are shown with the corresponding values of  $\alpha_{ref}$ ,  $\beta_{ref}$  and  $v_{ref}$  in Table 2 for 9 various experimental conditions. It should be noted that when  $\alpha_{ref} = 0^\circ$  then both  $\beta_{ref}$  and  $\beta_{meas}$  are meaningless (see figure 2).

It is clear from Table 2 that the values of  $\alpha_{meas}$ ,  $\beta_{meas}$  and  $v_{meas}$  as measured by the 4-sensor conductance probe are reasonably close to the reference values for these quantities. In fact, the mean error in  $\alpha_{meas}$  is  $1.32^\circ$ , the mean error in  $\beta_{meas}$  is  $-0.1^\circ$  and the mean percentage error in  $v_{meas}$  is 0.8%.

## 6. Conclusions

Both 4-sensor conductance probe and two high speed cameras were used to measure the polar angle, the azimuthal angle and the magnitude of the bubble velocity vector in a bubbly water tank. From the comparisons of both results it can be seen that the mean error in the bubble polar angle measured by the probe was  $1.32^\circ$ , the mean error in the bubble azimuthal angle measured by the probe was  $-0.1^\circ$  and the mean percentage error in the measured bubble velocity magnitude measured by the probe was 0.8%. The findings shows the best results yet obtained from a 4-sensor probe when measuring the velocity vectors of bubbles with a major axis of less than 10mm and a minor axis of about 5mm.

References:-

1. Mishra R., Lucas G. P., Kieckhofer H., "A model for obtaining the velocity vectors of spherical droplets in multiphase flows from measurements using an orthogonal four-sensor probe.", Meas. Sci. Technol. volume 13, pages 1488-1498, 2002.
2. Lucas G. P., Mishra R., "Measurement of bubble velocity components in a swirling gas-liquid pipe flow using a local four-sensor conductance probe.", Meas. Sci. Technol., volume 16, pages 749-758, 2004.
3. Panagiotopoulos N., Lucas G. "Simulation of a local four-sensor conductance probe using a rotating dual-sensor probe." Meas. Sci. Technol., volume 18, pages 2563-2569, 2007
4. Pradhan S., Lucas G., Panagiotopoulos N. "Sensitivity Analysis for a 4-Sensor Probe Used for Bubble Velocity Vector Measurement" Researchers conference University of Huddersfield 2006.
5. Hosgett S., Ishii M., "Local two-phase flow measurement using sensor techniques.", Nuclear engineering and design, volume 175, pages 15-24, 1997